The Journal Article: subtitle

Jonas Kersulis, Ian Hiskens
Elec. Eng. and Computer Science
University of Michigan
Ann Arbor, MI, United States

Michael Chertkov, Scott Backhaus
Center for Nonlinear Studies
Los Alamos National Laboratory
Los Alamos, NM, United States

Daniel Bienstock
Ind. Eng. and Operations Research
Columbia University
New York, NY, United States

***Abstract*—A previously-developed method for studying a transmission network's vulnerability to wind forecast inaccuracy is expanded. This method uses optimization to find a wind generation pattern close to the forecast that violates a specified line. Repeating the optimization for all lines in the network yields a set of generation patterns which may be sorted by likelihood. Instanton analysis thus yields insight into the potential effects of wind forecast inaccuracy at the system level.**

***Index Terms*—Forecast uncertainty, Optimization, Transmission operations, Wind energy**

I. Introduction and review

The impact of wind forecast inaccuracy is greater than ever in grids around the world. As reliance on wind generation increases, changes in weather can induce network congestion. In certain cases this congestion may even cause a transmission line to overheat and sag. System operators use wind forecast data to steer the network away from these scenarios, but wind forecasts are significantly less accurate than generation and demand predictions. How might forecast inaccuracies compound across the network to overheat transmission lines? How likely is this to occur? To help answer these questions we present temporal instanton analysis, which uses mathematical programming to find troublesome wind patterns and rank them according to likelihood. With this information, system operators and planners gain a new line of defense against renewable generation uncertainty.

The remainder of this paper is organized as follows. Section II translates the verbal description above into a mathematical formulation of temporal instanton analysis. Section III describes a previously-developed solution method for the temporal instanton problem. We expand on prior work by providing a more detailed treatment of the objective function, discussing implementation details including computational complexity and sparsity, and proposing a particular algorithm for solving the secular equation. Section IV contains results for two networks: a modified version of the RTS-96 and the larger WECC network. The former network has been used in previous instanton analysis studies, while the latter serves to demonstrate scalability of temporal instanton analysis. Finally, an appendix contains a detailed description of the thermal model used to calculate line temperature.

Wind forecasting is a complicated business. Consider first a single wind farm whose output is forecast for some future time. Let the forecast performance be represented by a random variable. Using historical data from ERCOT in Texas, [1] determined appropriate density functions for this variable based on the forecast horizon. For predictions a few minutes or hours away, forecast performance is approximately Cauchy, with deviations concentrated heavily around the forecast value. As the time horizon increases, accuracy suffers and the distribution approaches a Gaussian curve. Now consider several wind farms scattered across a transmission grid. In addition to individual site forecasts, one must now consider overall patterns. Wind sites tend to be spatially correlated: if wind speed increases at one site, it is unlikely that it will simultaneously decrease at a neighboring site. Temporal covariance further complicates matters: increased wind at site A now may be strongly correlated with greater wind speeds at site B in the future. Spatial and temporal covariance may be calculated from measurement data and encoded in a covariance matrix. The optimization framework developed in this paper contains such a covariance matrix in its objective function.

Suppose that wind generation throughout the network is represented as a Gaussian random vector. Comparing our objective function to the PDF of such a vector shows that Q_{dev} corresponds to the inverse of covariance.

II. Temporal instanton problem as a QCQP

A. Line losses

Starting with the AC line loss expression, [2] derived the following approximate relationship between line losses and voltage angle differences for line (i, j):

$$f_{ij}^{\text{loss}} \approx r_{ij} \left(\frac{\theta_{ij}}{x_{ij}} \right)^2. \tag{1}$$

In this expression, f_{ij}^{loss} is the approximate active power loss on the line; θ_{ij} is the difference between angles θ_i and θ_k; and $r_{ij} + jx_{ij}$ is the impedance of the line between nodes i and j. Three assumptions underpin (1): voltage magnitudes are all 1 pu, cosine may be approximated by its second-order Taylor

The authors acknowledge the support of the Los Alamos National Laboratory Grid Science Program, subcontract 270958.

expansion, and $x_{ij} \geq 4r_{ij}$. Thus, (1) uses DC power flow assumptions to approximate line losses, but remains nonlinear.

B. Objective function and Q_{obj}

The objective function depends solely on deviation variables, so Q_{obj} is a matrix that weights only the dev variables in z. If there are two time steps, for example, the vector of variables would be $z = \begin{bmatrix} dev_t^\top & \theta_1^\top & \alpha_1 & dev_2^\top & \theta_2^\top & \alpha_2 & \hat{\theta} \end{bmatrix}^\top$, and Q_{obj} would be,

$$Q_{obj} = \begin{bmatrix} Q_{dev} & 0 & 0 & 0 & 0 & 0 \\ 0 & 0 & 0 & 0 & 0 & 0 \\ 0 & 0 & 0 & 0 & 0 & 0 \\ 0 & 0 & 0 & Q_{dev} & 0 & 0 \\ 0 & 0 & 0 & 0 & 0 & 0 \\ 0 & 0 & 0 & 0 & 0 & 0 \end{bmatrix}.$$

Note that Q_{dev} represents covariance between wind-farms (if any). In the Section III numerical analysis, we will assume $Q_{dev} = I$, the identity matrix.

C. Linear constraints: A and b

All constraints except the temperature limit may be grouped into a single linear system $Az = b$. Setting aside the T auxiliary variables for the moment, the A matrix has a block diagonal structure where each block consists of $(N+1)$ rows and $(N_R + N)$ columns. The first N rows describe power balance and distributed slack behavior at each node. For node i and time t, we fix elements of A and b to establish

$$\sum_j Y_{ij}\theta_{j,t} = (G^0_{i,t} + k_i\alpha_t) + (R_{i,t} + dev_{i,t}) - D_{i,t}. \quad (2)$$

The first pair of terms on the right-hand side of (2) represents conventional generation with distributed slack (generator i is taking a portion k_i of the mismatch α_t). The second pair of terms is renewable generation: forecast $R_{i,t}$ plus deviation $dev_{i,t}$. The final term is demand at node i and time t. (Note that renewable generation terms are zero for nodes without wind-farms.) In addition to the N rows corresponding to (2) at the N nodes, there is one additional equation associated with time t that fixes the angle reference:

$$\theta_{ref,t} = 0. \quad (3)$$

The $(N+1)$ rows of $Az = b$ expressed in (2) and (3) pertain to a single time step t, with T blocks of this form arranged diagonally to form $(N+1)T$ rows of A and the corresponding b vector. There is one additional block of A used to define auxiliary angle difference variables $\hat{\theta}_{ij,t}$ in terms of angle variables $\theta_{i,t}$ and $\theta_{j,t}$ at each time step:

$$\hat{\theta}_{ij,t} = \tau^{\frac{T-t}{2}}(\theta_{i,t} - \theta_{j,t}) \ . \quad (4)$$

The next subsection explains why these variables are helpful.

D. Quadratic constraint: Q_θ and c

Recall that (43) describes the temperature constraint on a chosen line (i, j). We can rearrange (43) into the form of (44c), with all constants on the right side:

$$\boldsymbol{\theta}_{ij}^\top \boldsymbol{\tau}_{ij} \boldsymbol{\theta}_{ij} = \frac{x_{ij}^2}{\rho_{ij} r_{ij}} \left(\Delta T_{ij}^{\lim} - \delta_{ij} \boldsymbol{\Delta} \boldsymbol{d}_{ij}^\top \boldsymbol{\tau}_{ij} \mathbf{1} \right) \quad (5)$$

This makes it clear that the appropriate value of c in (44c) is

$$c = \frac{x_{ij}^2}{\rho_{ij} r_{ij}} \left(\Delta T_{ij}^{\lim} - \delta_{ij} \boldsymbol{\Delta} \boldsymbol{d}_{ij}^\top \boldsymbol{\tau}_{ij} \mathbf{1} \right) \quad (6)$$

From the definition of $\hat{\theta}_{ij,t}$ in (4), we see that the left side of (5) may be expressed as $\hat{\theta}_{ij}^\top \hat{\theta}_{ij}$. Thus, if the $\hat{\theta}_{ij}$ variables are placed at the bottom of z, Q_θ must be a matrix of zeros with a T-by-T identity matrix in the lower-right corner. This ensures that $z^\top Q_\theta z = \hat{\theta}_{ij}^\top \hat{\theta}_{ij}$, as desired.

Section **??** described the temporal instanton problem, Section IX expressed it as a QCQP, and this section defined each component. Next we present a solution method for (44).

III. Solution method and implementation details

The structure of (44) is similar to that of the well-known trust region subproblem. Here we describe a four-step solution method based in part on [3]. We begin by considering the vector of variables z as three groups: $z_1 \in \mathbb{R}^{N_R T}$ contains all wind deviations, $z_2 \in \mathbb{R}^{(N+1)T}$ contains angle and mismatch variables, and $z_3 \in \mathbb{R}^T$ contains auxiliary angle difference variables involved in line temperature calculation. (This partition of z is independent of how the variables are ordered.) With this notation, the problem becomes

$$\begin{aligned} \min \quad & z_1^\top Q_z z_1 && (7a) \\ s.t. \quad & Az = b && (7b) \\ & z_3^\top z_3 = c, && (7c) \end{aligned}$$

where Q_z is Q_{dev} repeated in block-diagonal fashion T times.

Several changes of variables may be used to obtain an equivalent form of (7) whose solution is straightforward.

A. Translation

The first step is to change variables from z to $y = z - z^*$, where $z^* \in \{z : Az = b\}$. This translation transforms $Az = b$ into $Ay = 0$. To prevent the change from introducing a linear term into the quadratic constraint, we require $z_3^* = 0$. To satisfy $Az^* = b$, the subvectors z_1^* and z_2^* must satisfy,

$$A \begin{bmatrix} z_1^* \\ z_2^* \\ 0 \end{bmatrix} = b.$$

It is straightforward to find a min-norm z^* that satisfies this constraint by partitioning and factorizing A appropriately. After translation, the problem becomes

$$\begin{aligned} \min \quad & y_1^\top Q_z y_1 + 2 y_1^\top Q_z z_1^* && (8a) \\ s.t. \quad & Ay = 0 && (8b) \\ & y_3^\top y_3 = c. && (8c) \end{aligned}$$

B. Kernel mapping

The form of (8b) suggests an intuitive explanation: any solution to (8) must lie in the nullspace (kernel) of A. If $\dim \mathcal{N}(A) = k$ is the dimension of this nullspace, we can let $y = Nx$ where the k columns of N span $\mathcal{N}(A)$. (Note that x does not refer to reactance in this context.) This change of variables is akin to a rotation, but reduces the problem dimension to k. Partitioning N according to,

$$\begin{bmatrix} y_1 \\ y_2 \\ y_3 \end{bmatrix} = \begin{bmatrix} N_1 \\ N_2 \\ N_3 \end{bmatrix} x$$

allows (8) to be written,

$$\begin{aligned} \min \quad & x^\top (N_1^\top Q_z N_1) x + 2x^\top (N_1^\top Q_z z_1^*) && \text{(9a)} \\ s.t. \quad & x^\top N_3^\top N_3 x = c. && \text{(9b)} \end{aligned}$$

All feasible solutions to (9) lie in the nullspace of A, so the linear constraints are now implicit.

C. Obtaining a norm constraint

After kernel mapping, the quadratic constraint is no longer a norm constraint. This can be corrected in two steps. First, perform an eigendecomposition $N_3^\top N_3 = UDU^\top$ and let $\hat{x} = U^\top x$. The constraint is diagonal in terms of $\hat{x}$:

$$x^\top N_3^\top N_3 x = \hat{x}^\top D \hat{x} \tag{10}$$

where D is diagonal and has at most T nonzero elements, so the right side of (10) may be expanded into:

$$\begin{bmatrix} \hat{x}_1^\top & \hat{x}_2^\top \end{bmatrix} \begin{bmatrix} 0 & 0 \\ 0 & \hat{D} \end{bmatrix} \begin{bmatrix} \hat{x}_1 \\ \hat{x}_2 \end{bmatrix}. \tag{11}$$

The second step is to change variables from $\hat{x}$ to $w = [w_1^\top \; w_2^\top]^\top$. The variables x, $\hat{x}$ and w are related through:

$$\begin{aligned} \begin{bmatrix} w_1 \\ w_2 \end{bmatrix} &= \begin{bmatrix} I & 0 \\ 0 & \hat{D}^{1/2} \end{bmatrix} \begin{bmatrix} \hat{x}_1 \\ \hat{x}_2 \end{bmatrix} = K\hat{x} && \text{(12)} \\ \implies w &= KU^\top x. \end{aligned}$$

(Note that $x = UK^{-1}w$ because $UU^\top = I$.) In terms of w, (9b) is transformed through (10) to give the form of a norm:

$$\hat{x}^\top D \hat{x} = \hat{x}_2^\top \hat{D}^{1/2} \hat{D}^{1/2} \hat{x}_2 = w_2^\top w_2 \; . \tag{13}$$

Of course, this change of variables must also be applied to the cost function. After substitution and simplification, the full problem becomes:

$$\begin{aligned} \min \quad & w^\top B w + w^\top b && \text{(14a)} \\ s.t. \quad & w_2^\top w_2 = c && \text{(14b)} \end{aligned}$$

where

$$B = K^{-1}U^\top N_1^\top Q_z N_1 U K^{-1} \text{ and } b = 2K^{-1}U^\top N_1^\top Q_z z_1^*.$$

The manipulations in this section have restored the norm structure of the quadratic constraint. In the next section we use the KKT conditions of (14) to eliminate w_1, the unconstrained part of w. This will allow us to write the objective in terms of w_2 only.

D. Eliminating w_1

Note that w_1 is unconstrained in (14). For a fixed w_2, we can use the KKT conditions to find w_1 such that the objective is minimized. Begin by expanding the objective:

$$\begin{aligned} f(w) &= \begin{bmatrix} w_1^\top & w_2^\top \end{bmatrix} \begin{bmatrix} B_{11} & B_{12} \\ B_{12}^\top & B_{22} \end{bmatrix} \begin{bmatrix} w_1 \\ w_2 \end{bmatrix} + \begin{bmatrix} w_1^\top & w_2^\top \end{bmatrix} \begin{bmatrix} b_1 \\ b_2 \end{bmatrix} \\ &= w_1^\top B_{11} w_1 + 2w_1^\top B_{12} w_2 + w_2^\top B_{22} w_2 \\ &\quad + w_1^\top b_1 + w_2^\top b_2. \end{aligned}$$

Next, set the partial derivative with respect to w_1 equal to zero:

$$\begin{aligned} \frac{\partial f}{\partial w_1} &= 2w_1^\top B_{11} + 2w_2^\top B_{12}^\top + b_1^\top = 0 \\ \implies w_1 &= -B_{11}^{-1} \left(B_{12} w_2 + \frac{1}{2} b_1 \right). && \text{(15)} \end{aligned}$$

After substitution of (15), the objective depends only on w_2:

$$\begin{aligned} f(w_2) = w_2^\top &\left(B_{22} - B_{12}^\top B_{11}^{-1} B_{12} \right) w_2 \\ &+ w_2^\top (b_2 - B_{12}^\top B_{11}^{-1} b_1). \end{aligned}$$

(Note that the constant term, which plays no role in minimization, was omitted.) The full optimization problem becomes:

$$\begin{aligned} \min \quad & w_2^\top \hat{B} w_2 + w_2^\top \hat{b} && \text{(16a)} \\ s.t. \quad & w_2^\top w_2 = c, && \text{(16b)} \end{aligned}$$

where

$$\hat{B} = B_{22} - B_{12}^\top B_{11}^{-1} B_{12} \text{ and } \hat{b} = b_2 - B_{12}^\top B_{11}^{-1} b_1.$$

This is a QCQP in T dimensions with a single norm constraint. It is straightforward to obtain solutions to this problem, as the next subsection shows.

E. Solution via enumeration

A straightforward method of solving (16) involves initially diagonalizing $\hat{B}$ through an eigendecomposition. It will be assumed that step has been completed.

Let v be the Lagrange multiplier associated with (16b) and write the first-order optimality condition for (16):

$$\begin{aligned} \frac{\partial \mathcal{L}(w_2, v)}{\partial w_2} &= 2\hat{B} w_2 + \hat{b} - v(2w_2) = 0 \\ \implies \hat{B} w_2 + \frac{1}{2} \hat{b} &= v w_2. && \text{(17)} \end{aligned}$$

Equation (17) is a linear system that yields w_2 for fixed v:

$$w_{2,i} = \frac{\hat{b}_i / 2}{v - \hat{B}_{i,i}}. \tag{18}$$

In addition to satisfying (18), an optimal w_2 must satisfy the quadratic constraint. Substituting (18) into (16b) yields the "secular equation" (see [3]):

$$s(v) = \sum_i \left(\frac{\hat{b}_i / 2}{v - \hat{B}_{i,i}} \right)^2 = c. \tag{19}$$

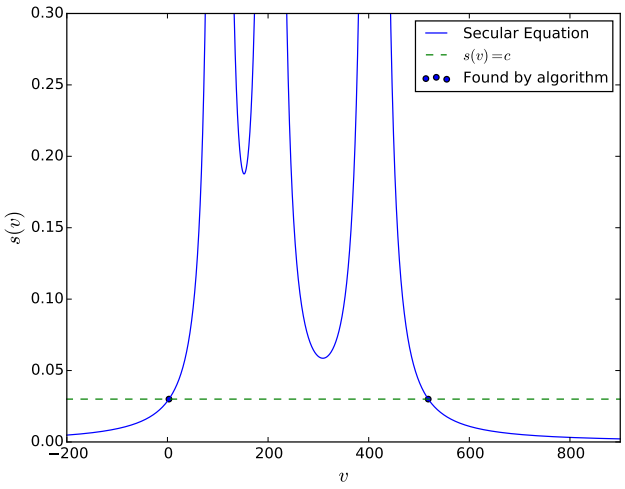

Fig. 1. Plot of secular equation for a single line in the RTS-96. Note that $s(v)$ approaches infinity at the three poles, and there could be as many as six solutions if c were large enough.

Note that $s(v)$ has one pole per unique nonzero diagonal element of $\hat{B}$. There are at most two solutions per pole, one on each side. This is best understood graphically. Figure 1 illustrates a three-pole secular equation taken from analysis of the RTS-96 network. The Lagrange multiplier v is on the horizontal axis, and the secular equation value $s(v)$ is on the vertical. Solutions are intersections of $s(v)$ with the horizontal line $s(v) = c$. They can be computed numerically with a simple binary search algorithm.

F. Computation complexity

G. Sparsity

IV. Results

We used data from [4] to demonstrate temporal instanton analysis on a wind-augmented RTS-96 network model. Consider a scenario unfolding over three time steps: first the wind forecast is 50% of some nominal value, next it is equal to the nominal value, and finally it is scaled to 150% of nominal. Throughout this wind ramping, generator dispatch and demand remain constant. Temporal instanton analysis with $c = 0.03$ and $\tau = 0.5$ indicates that the line between buses 121 and 325 is most susceptible to excessive heating under these conditions. In other words, of all dangerous wind patterns that could occur during the wind ramp, the most likely is a pattern that overheats the line between buses 121 and 325. Figure 1 illustrates the secular equation used to find this instanton pattern, and Figure 2 shows the system state at the second time step. The largest deviation in the instanton pattern is 0.73 pu, well within the range of wind forecast values (whose maximum is 1.2 pu).

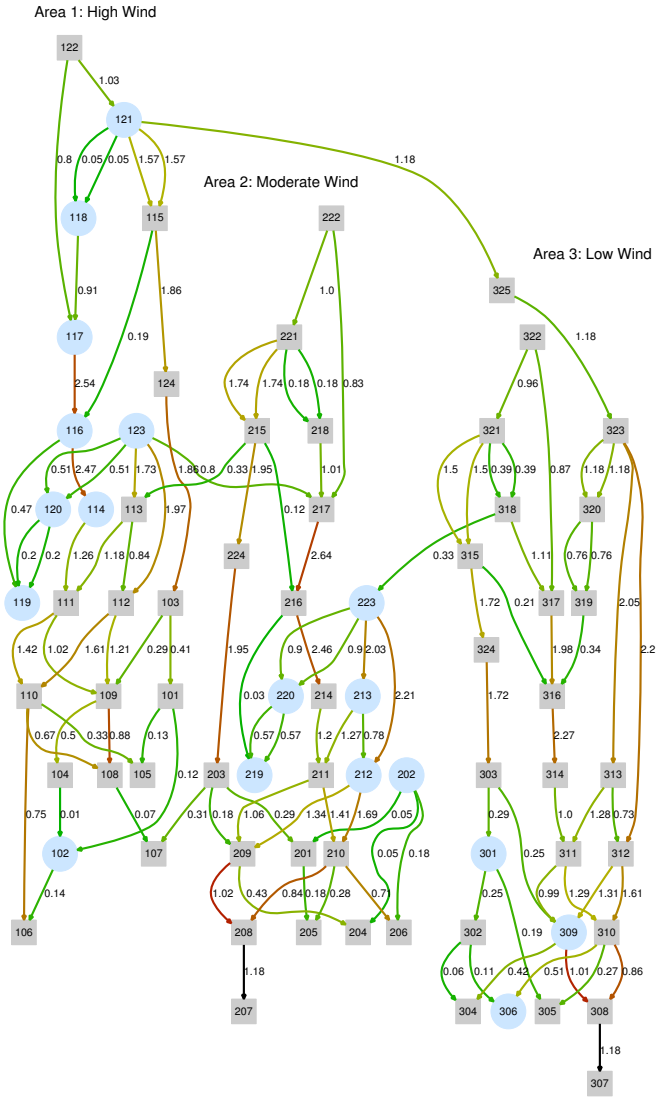

Fig. 2. Graph depiction of RTS-96 system state under instanton conditions at time step 2 of 3. The stressed line is between buses 121 and 325 (top center). wind-farms are indicated by blue, and lines are colored according to how close their flows are to static active power limits.

V. Conclusions

VI. Appendix: Line temperature model

A. The heat balance equation

The change in temperature of any object may be expressed as a differential equation called the heat balance equation. This equation relates temperature change to a sum of various sources of heating. The IEEE 738 standard [5] provides the following heat balance equation for a transmission line:

$$\frac{dT}{dt} = \frac{1}{m \cdot C_p}\left[I^2 \cdot R(T) - q_c - q_r + q_s\right] \qquad (20)$$

where

- T is the conductor average temperature.

- $m \cdot C_p$ is the product of mass and heat capacity.
- $I^2 \cdot R(T)$ represents heat rate due to resistive heating. In this paper the term is replaced by f_{ij}^{loss}, the DC approximate line loss expression derived in [2].
- q_c is the rate of heat loss due to convection. Any object at a higher temperature than surrounding air will gradually cool as the air carries heat away. This phenomenon is proportional to the temperature difference between the line and surrounding air:

$$q_c = \eta_c \cdot (T - T_{\text{amb}}) \ , \tag{21}$$

  where T_{amb} is the ambient temperature (of surrounding air).
- q_r is the rate of heat loss due to radiation. Thermal radiation is the process by which thermal energy is converted to electromagnetic energy in all objects with non-zero absolute temperature. It is modeled by a fourth-order expression:

$$q_r = \eta_r \cdot \left[(T + 273)^4 - (T_{\text{amb}} + 273)^4\right] \tag{22}$$

- q_s is the rate of heat gain due to solar heating. In this paper the solar heat rate is fixed to some conservative constant (representing full direct sun), but it is important to note that solar heat rate varies significantly with cloud cover, geometry, and even insulation type (reflective versus black).

B. Linearization of radiation heat rate

When (20) is combined with an initial temperature T_0, the resulting initial value problem makes it possible to determine the temperature at any later time. Let's substitute the DC loss approximation, (21), and (22) into (20) and attempt to solve for temperature:

$$\frac{dT}{dt} = \frac{1}{mC_p}\big[f_{ij}^{\text{loss}} - \eta_c\left(T(t) - T_{\text{amb}}\right) - \eta_r\left((T(t) + 273)^4 - (T_{\text{amb}} + 273)^4\right) + q_s\big] \tag{23}$$

Suppose that power flow, ambient temperature, and solar heat rate are constant during a temperature change calculation. There are just two variable terms on the right-hand side: one first-order, one fourth-order. The fourth-order term (which comes from q_r) makes this equation difficult to solve. Fortunately, q_r is approximately linear over the temperature range we are interested in (from ambient to line limit). The figure below compares q_r to a conservative[1] linearization $\tilde{q}_r$.

The green trace is the linearization of q_r about T_{mid}, the midpoint between the ambient and limit temperatures. Let's replace q_r by this linear approximation $\tilde{q}_r$:

$$\frac{dT}{dt} = \frac{1}{mC_p}\left[f_{ij}^{\text{loss}} - \eta_c\left(T(t) - T_{\text{amb}}\right) - \tilde{q}_r + q_s\right] \tag{24}$$

[1]Because a transmission line is hotter than surrounding air, radiation tends to decrease line temperature. Thus, a conservative approach will underestimate the radiation heat rate, leading to slightly higher temperatures.

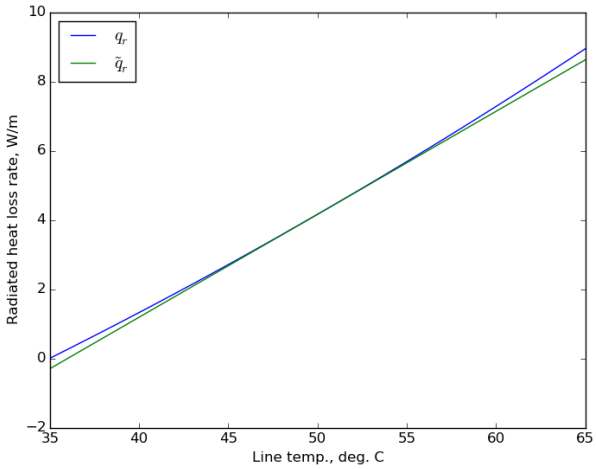

Fig. 3. Comparison of fourth-order radiation heat rate q_r (22) with conservative linearization $\tilde{q}_r$ across a range of temperatures. Ambient temperature is 35°C and the conductor thermal limit is 65°C.

where

$$\tilde{q}_r = \eta_r\left((T_{\text{mid}} + 273)^4 - (T_{\text{amb}} + 273)^4\right) + 4\eta_r(T_{\text{mid}} + 273)^3 \cdot (T(t) - T_{\text{m}} \tag{25}$$

C. Line temperature as IVP solution

After simplification, (24) becomes

$$\frac{dT}{dt} = aT(t) + b \tag{26}$$

where constants a and b are defined as

$$a = \frac{1}{mC_p}\left[-\eta_c - 4\eta_r(T_{\text{mid}} + 273)^3\right] \tag{27a}$$

$$b = \frac{1}{mC_p}\left[f_{ij}^{\text{loss}} + \eta_c T_{\text{amb}} - \eta_r\left((T_{\text{mid}} + 273)^4 - (T_{\text{amb}} + 273)^4\right) + 4\eta_r T_{\text{m}}\right. \tag{27b}$$

The differential equation (26) has a straightforward solution:

$$T(t) = ke^{at} - \frac{b}{a} \tag{28}$$

where $k = T(0) + b/a$. Note that b is influenced by power flow (via f_{ij}^{loss}), but a is not.

VII. From Temperature Equation to Optimization Constraint

The important thing to note about the temperature equation (28) is that it is influenced only by initial temperature and the angle difference during each time interval. There is therefore a recursive relationship between final temperature and initial temperature that involves only angle differences.

A. Recursive relationship between final and initial temperatures

Suppose there are three time intervals: t_1, t_2, and t_3. Then the line temperature at the end of the third interval is given by

$$\begin{aligned} T(t_3) &= k_3 e^{(t_3-t_2)a} - \frac{b_3}{a} \\ &= \left[k_2 e^{(t_2-t_1)a} - \frac{b_2}{a} + \frac{b_3}{a}\right] e^{(t_3-t_2)a} - \frac{b_3}{a} \\ &= \left[\left(T(t_1) + \frac{b_2}{a}\right) e^{(t_2-t_1)a} - \frac{b_2}{a} + \frac{b_3}{a}\right] e^{(t_3-t_2)a} - \frac{b_3}{a} \\ &= \left\{\left[\left(T(t_0) + \frac{b_1}{a}\right) e^{(t_1-t_0)a} - \frac{b_1}{a} + \frac{b_2}{a}\right] e^{(t_2-t_1)a} - \frac{b_2}{a} + \frac{b_3}{a}\right\} e^{(t_3-t_2)a} - \frac{b_3}{a} \end{aligned} \tag{29}$$

The recursive pattern is apparent. Because all time intervals are the same length, we have

$$e^{(t_3-t_2)a} = e^{(t_2-t_1)a} = e^{(t_1-t_0)a} ,$$

and we can distribute in (29) to obtain

$$T(t_3) = (e^{(t_1-t_0)a})^3 \left(T(t_0) + \frac{b_1}{a}\right) + (e^{(t_1-t_0)a})^2 \left(-\frac{b_1}{a} + \frac{b_2}{a}\right) + (e^{(t_1-t_0)a}) \left(-\frac{b_2}{a} + \frac{b_3}{a}\right) - \frac{b_3}{a} \tag{30}$$

Because power flow data enters through b_1, b_2, and b_3, it makes sense to group terms accordingly:

$$\begin{aligned} T(t_3) = ((e^{(t_1-t_0)a})^3 T(t_0) &+ \left(\frac{(e^{(t_1-t_0)a})^3}{a} - \frac{(e^{(t_1-t_0)a})^2}{a}\right) b_1 + \\ + \left(\frac{(e^{(t_1-t_0)a})^2}{a} - \frac{(e^{(t_1-t_0)a})^1}{a}\right) b_2 &+ \left(\frac{e^{(t_1-t_0)a}}{a} - \frac{1}{a}\right) b_3 \end{aligned} \tag{31}$$

The pattern in the above expression makes it easy to extend $T(t_3)$ to cover the general case $T(t_n)$:

$$T(t_n) = (e^{(t_1-t_0)a})^n T(t_0) + \frac{1}{a} \sum_{i=1}^{n} \left((e^{(t_1-t_0)a})^i - (e^{(t_1-t_0)a})^{i-1}\right) b_{n-i+1} \tag{32}$$

Ultimately (32) will be used to constrain a line's final temperature to some limiting value. The remainder of this section will relate (32) back to power flow angles so it can be "plugged in" to the optimization framework.

B. Relating temperature to angle differences

Recall that b_n depends on the angle difference at time t_n:

$$\begin{aligned} b_n &= \frac{1}{mC_p}\left[\frac{r_{ij}}{x_{ij}^2} \cdot \frac{S_b}{3L_{ij}} \theta_{ij}(t_n)^2 + \eta_c T_{\text{amb}} - \eta_r \left((T_{\text{mid}} + 273)^4 - (T_{\text{amb}} + 273)^4\right) + 4\eta_r T_{\text{mid}} (T_{\text{mid}} + 273)^3\right] \\ b_n &= c\theta_{ij}(t_n)^2 + d \end{aligned} \tag{33}$$

where constants c and d are defined as:

$$c = \frac{r_{ij} S_b}{3mC_p x_{ij}^2 L_{ij}}$$

$$d = \frac{1}{mC_p}\left[\eta_c T_{\text{amb}} - \eta_r \left((T_{\text{mid}} + 273)^4 - (T_{\text{amb}} + 273)^4\right) + 4\eta_r T_{\text{mid}} (T_{\text{mid}}\right.$$

Substitute (33) into (32):

$$T(t_n) = (e^{(t_1-t_0)a})^n T(t_0) + \frac{1}{a} \sum_{i=1}^{n} \left((e^{(t_1-t_0)a})^i - (e^{(t_1-t_0)a})^{i-1}\right) (c\theta_{ij}($$

Expand the sum term:

$$\begin{aligned} \frac{1}{a} \sum_{i=1}^{n} \left((e^{(t_1-t_0)a})^i - (e^{(t_1-t_0)a})^{i-1}\right) (c\theta_{ij}(t_{n-i+1})^2 + d) = \frac{c}{a}\left[\sum_{i=1}^{n} \left((e\right.\right. \\ + \frac{d}{a}\left[\sum_{i=1}^{n} \left((e^{(t_1-t_0)a})^i - (e^{(t_1-t_0)a})^{i-1}\right)\right] \end{aligned} \tag{34}$$

Substitute (34) into the line temperature equation, introducing the constant f to keep things a bit neater:

$$T(t_n) = f + \frac{c}{a}\left[\sum_{i=1}^{n} \left((e^{(t_1-t_0)a})^i - (e^{(t_1-t_0)a})^{i-1}\right) \theta_{ij}(t_{n-i+1})^2\right] \tag{35}$$

where

$$f = (e^{(t_1-t_0)a})^n T(t_0) + \frac{d}{a}\left[\sum_{i=1}^{n} \left((e^{(t_1-t_0)a})^i - (e^{(t_1-t_0)a})^{i-1}\right)\right] \tag{36}$$

Rearrange (35) to isolate angle differences:

$$\sum_{i=1}^{n} \left((e^{(t_1-t_0)a})^i - (e^{(t_1-t_0)a})^{i-1}\right) \theta_{ij}(t_{n-i+1})^2 = \frac{a}{c}(T(t_n) - f) \tag{37}$$

Now define

$$\hat{\theta}_{ij}(t_k) = \theta_{ij}(t_k) \sqrt{(e^{(t_1-t_0)a})^{n-k+1} - (e^{(t_1-t_0)a})^{n-k}} \tag{38}$$

to obtain

$$\sum_{k=1}^{n} \hat{\theta}_{ij}(t_k)^2 = \frac{a}{c}\left(T(t_n) - f\right) \tag{39}$$

The expression (39) may be used to constrain line temperature to be equal to some limiting value by the end of the last time interval.

This derivation has been somewhat messy. The line temperature constraint is summarized in the next section for convenience.

C. Summary of line temperature constraint

Suppose our time horizon consists of n intervals, each on the order of ten minutes long. Power flow data is updated after each interval, but all other parameters remain constant. Choose a single transmission line in the network, and suppose it lies between nodes i and j. This line has a thermal limit of T_{lim}

(°C). We can constrain the line's temperature to be equal to this limiting value by enforcing the second-order constraint:

$$\sum_{k=1}^{n} \hat{\theta}_{ij}(t_k)^2 = \frac{a}{c}\left(T_{\text{lim}} - f\right) \tag{40}$$

where

- $\hat{\theta}_{ij}(t_k) = \theta_{ij}(t_k)\sqrt{(e^{(t_1-t_0)a})^{n-k+1} - (e^{(t_1-t_0)a})^{n-k}}$
  - $\theta_{ij}(t_k)$ is the angle difference across line ij at time interval t_k.
  - $(t_1 - t_0)$ is the length of each time interval (in seconds)
- $a = \frac{1}{mC_p}\left[-\eta_c - 4\eta_r(T_{\text{mid}} + 273)^3\right]$ is constant with units of s^{-1}
  - mC_p is the heat capacity, with units of J/m-°C
  - η_c is the conductive heat loss rate coefficient, with units of W/m-°C
  - η_r is the conductive heat loss rate coefficient, with units of W/m-°C[4]
  - T_{mid} is the average of ambient temperature T_{amb} and limit temperature T_{lim}, in Celsius
- $c = \frac{r_{ij}S_b}{3mC_p x_{ij}^2 L_{ij}}$ is a constant with units of W/m
  - r_{ij} is resistance of line ij in per unit
  - x_{ij} is reactance of line ij in per unit
  - S_b is the system base (e.g. 100 MVA)
  - L_{ij} is the length of one phase of line ij, in m
- $f = (e^{(t_1-t_0)a})^n T(t_0) + \frac{d}{a}\left[\sum_{i=1}^{n}\left((e^{(t_1-t_0)a})^i - (e^{(t_1-t_0)a})^{i-1}\right)\right]$ is a constant with units of degrees Celsius
  - $T(t_0)$ is the line's initial temperature (steady state temperature under base case power flow condition)
  - $d = \frac{1}{mC_p}\left[\eta_c T_{\text{amb}} - \eta_r\left((T_{\text{mid}} + 273)^4 - (T_{\text{amb}} + 273)^4\right.\right.$ is a constant with units of W/m
    - q_s is the solar heat gain rate in W/m

VIII. Numerical comparison to IEEE 738 standard model

To validate the approximate line temperature model derived here, I compared it to the IEEE 738 standard model using RTS-96 and Waxwing conductor parameters.

A. Summary of IEEE 738 temperature calculation

IEEE recommends numerically integrating (20) to compute temperature changes. The temporal instanton framework uses approximate DC losses in place of $I^2R(T_{\text{avg}})$, so we will be integrating the following heat balance equation:

$$\frac{dT_{\text{avg}}}{dt} = \frac{1}{mC_p}\left(r_{ij}\frac{\theta_{ij}^2}{x_{ij}^2}\frac{S_b}{3L_{ij}} - q_c - q_r + q_s\right) \tag{41}$$

Heat rates q_c and q_r are calculated according to (21) and (22), respectively (copied here for convenience):

$$q_c = \eta_c \cdot (T - T_{\text{amb}})$$
$$q_r = \eta_r \cdot ((T + 273)^4 - (T_{\text{amb}} + 273)^4)$$

All other parameters are constant during temperature calculation. The important thing to keep in mind about IEEE 738 temperature calculation is that it requires numerical integration; there is no analytic temperature solution for (41). This means one must select an integration time step Δt. For each step, one computes the change in temperature by multiplying Δt by the value of (41) computed at that step. IEEE recommends a step size smaller than 10% of the conductor thermal time constant[2]. A smaller integration step size yields more accurate results.

B. Comparison

I used RTS-96 network data and Waxwing conductor parameters to compare IEEE 738 standard temperature calculation to the model derived in Section **??**. Figure 4 shows line temperatures calculated across three ten-minute time intervals, where each interval has a different angle difference (power flow). The angle differences are

Interval	Angle difference (rad)
1	0.09
2	0.04
3	0.15

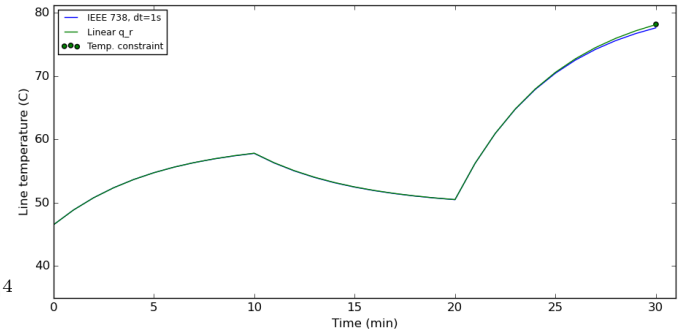

Fig. 4. Comparison of IEEE 738 and approximate temperature calculation methods

The blue trace in Figure 4 results from numerical integration of (41) with a 1s step size. The green trace comes from the approximate model derived in Section **??**. The green dot is the final temperature computed by (35).

Notes:

- Because the approximate line temperature model is analytic (Equation (28) is continuous) while the 738 model requires numerical integration, I chose a very small integration step size of one second to facilitate comparison.
- Because the approximate model underestimates the radiative heat loss rate (see Figure 3), the green trace should lie slightly above the blue one. This makes the approximate model conservative, which is desirable in the temporal instanton setting. Figure 4 illustrates this conservative behavior: the green trace lies on or above the blue trace throughout the time horizon.

[2]A typical transmission line thermal time constant is ten minutes, which means IEEE recommends an integration step size of one minute

TABLE I
LINE HEATING PARAMETERS

Parameter	Units	Description
T_s	s	Sample time
mC_p	$J/(m \cdot C)$	Per-unit-length heat capacity of the conductor
η_c	$W/(m \cdot C)$	Conductive heat loss rate coefficient
η_r	$W/(m \cdot C)$	Radiative heat loss rate coefficient
T^{lim}	C	Line temperature at steady-state current limit.
$\Delta q_{s,ij}$	W/m	Solar heat input into conductor
ΔT_{amb}	C	Change in ambient temperature

- The green dot, computed by (35), lies on top of the green curve. This validates the temperature constraint formulation (40).

C. Line temperature dynamics

D. Instanton formulation

The preceding discussion developed an approximate line loss expression to relate line temperature to angle variables according to (**??**). Here we describe the remaining parts of the temporal instanton model.

The following equations describe an optimization problem that minimizes deviation from the wind forecast while heating a certain line to a specified (limiting) temperature:

$$\min_{dev} \quad \sum_{t=1}^{T} dev_t^\top Q_{dev} dev_t \tag{42a}$$

subject to:

$$\sum_j Y_{ij}\theta_{ij,t} = G_{i,t} + R_{i,t} + dev_{i,t} - D_{i,t} \qquad \forall i \in 1...N,\ t \in 1...T \tag{42b}$$

$$G_t = G_{0,t} + k\alpha_t \qquad \forall t \in 1 \dots T \tag{42c}$$

$$\theta_{ref,t} = 0 \qquad \forall t \in 1 \dots T \tag{42d}$$

$$\Delta T_{ij}[T] = \Delta T_{ij}^{\text{lim}} \qquad \text{for some } (i,j) \in \mathcal{G} \tag{42e}$$

where:

- $dev_{i,t}$ is the difference between actual output and forecast output at wind-farm i and time t. Thus, dev_t is the vector of wind forecast deviations at time t.
- Q_{dev} may be set to the identity matrix or used to covariance between wind sites.
- $R_{i,t}$ is renewable generation forecast at bus i and time t.
- Y_{ij} is the (i,j)-th element of the admittance matrix, which assumes zero resistance.
- $\theta_{ij,t}$ is the difference between voltage angles θ_i and θ_j at time t.
- $G_{i,t}$ is conventional active power generation at node i and time t, and G_t is a vector including all nodes.
- $D_{i,t}$ is active power demand at bus i and time t.
- N is the number of buses (nodes).
- $G_{0,t}$ is scheduled conventional active power generation (without droop response).
- k is the vector of participation factors for conventional generators, with $\sum_i k_i = 1$. (The case where $k_i = 1$ corresponds to generator i taking all slack.)
- α_t is the power mismatch at time t.
- ΔT_{ij}^{lim} is the change in temperature that will push line (i,j) to its thermal limit.
- θ_{ref} is the voltage angle of the reference bus.
- $\mathcal{G}$ is the set of edges (lines).

Equation (42a) expresses the desire to find wind patterns that remain close to the wind forecast. The first constraint equation (42b) enforces DC power balance. The next constraint (42c) models conventional active power generation as a sum of scheduled generation and droop response (where generators share the task of compensating for mismatch between total generation and load). The system angle reference is established by (42d). Last is (42e), which constrains the temperature of a particular line to be equal to its limit at the final time T. Using (**??**) we can express (42e) as

$$\Delta T_{ij}^{\text{lim}} - \delta_{ij} \boldsymbol{\Delta} \boldsymbol{d}_{ij}^\top \boldsymbol{\tau}_{ij} \mathbf{1} = \frac{\rho_{ij} r_{ij}}{x_{ij}^2} \boldsymbol{\theta}_{ij}^\top \boldsymbol{\tau}_{ij} \boldsymbol{\theta}_{ij}. \tag{43}$$

Thus, (42) has a quadratic objective function, a set of linear constraints, and a single quadratic constraint. By solving (42) for each line in the network, we obtain a set of instanton candidate wind patterns, each of which will heat a particular line to its thermal limit. Of these candidates, the one that deviates least from the wind forecast (across all time steps) is the instanton wind pattern.

The form of (42) suggests a QCQP optimization formulation. The next section establishes this QCQP.

IX. Conversion to optimization problem

Previous instanton work relied on convex optimization to quickly find instanton wind patterns. Heat-constrained temporal instanton analysis is more complicated: it cannot be formulated as anything simpler than a quadratically-constrained quadratic program (QCQP). QCQPs are NP-hard in general; reasonable solutions may exist, but unless the quadratic constraint matrices are positive-definite there is no solution guarantee (see [6]). Because system operators require robustness, "no solution found" is an unacceptable output. With this criterion in mind, we proceed to develop an optimization model whose structure permits us to find solutions despite nonconvexity.

With all deviation, angle, and mismatch variables stacked into a single vector, (42) takes the form:

$$\min \quad z^\top Q_{obj} z \tag{44a}$$

$$s.t. \quad Az = b \tag{44b}$$

$$z^\top Q_\theta z = c. \tag{44c}$$

The objective (44a) is equivalent to (42a), the linear equality constraints (44b) represent (42b)-(42d), and the quadratic equality constraint (44c) is equivalent to (42e). The vector z

consists of $(N + N_R + 2)T$ variables, where N is the number of nodes, N_R is the number of nodes with wind-farms, and T is the number of time steps. Note that $N_R T$ of the variables represent deviations from forecast at each wind-farm and time step. There are also NT angle variables (of which T are fixed to zero according to (42d)) and T mismatch variables α_t (one per time step). The last T variables are auxiliary angle difference variables used to convert (42e) into a norm constraint; they are defined later in (4).

Variables may be stacked in any order. One convenient ordering is T groups of $(N + N_R + 1)$ variables, with the T auxiliary angle difference variables at the end. At a particular time step t, the group of $(N + N_R + 1)$ variables is $[dev_t^\top \quad \theta_t^\top \quad \alpha_t]^\top$, with dev_t representing deviations from forecast at the N_R wind nodes, θ_t is the column of N angle variables at time t, and α_t is the mismatch between generation and demand at time t.

The remainder of this section describes the components of (44). The objective matrix Q_{obj} is described in Section II-B, linear constraint parameters A and b are considered in Section II-C, and the constraint matrix Q_θ is addressed in Section II-D.

REFERENCES

[1] B. Hodge and M. Milligan, "Wind power forecasting error distributions over multiple timescales," in *2011 IEEE Power and Energy Society General Meeting*, Jul. 2011, pp. 1–8.

[2] M. Almassalkhi and I. Hiskens, "Model-predictive cascade mitigation in electric power systems with storage and renewables – part I: Theory and implementation," *IEEE Transactions on Power Systems*, vol. PP, no. 99, pp. 1–11, 2014.

[3] D. Bienstock and A. Michalka, "Polynomial Solvability of Variants of the Trust-region Subproblem," in *Proceedings of the Twenty-Fifth Annual ACM-SIAM Symposium on Discrete Algorithms*, ser. SODA '14. Portland, Oregon: SIAM, 2014, pp. 380–390. [Online]. Available: http://dl.acm.org/citation.cfm?id=2634074.2634102

[4] H. Pandzic, Y. Dvorkin, T. Qiu, Y. Wang, and D. Kirschen. Unit Commitment under Uncertainty - GAMS Models, Library of the Renewable Energy Analysis Lab (REAL), University of Washington, Seattle, USA. [Online]. Available: http://www.ee.washington.edu/research/real/gams_code.html

[5] "IEEE Standard for Calculating the Current-Temperature Relationship of Bare Overhead Conductors," *IEEE Std 738-2012 (Revision of IEEE Std 738-2006 - Incorporates IEEE Std 738-2012 Cor 1-2013)*, pp. 1–72, Dec. 2013.

[6] O. Mehanna, K. Huang, B. Gopalakrishnan, A. Konar, and N. Sidiropoulos, "Feasible point pursuit and successive approximation of non-convex QCQPs," *IEEE Signal Processing Letters*, vol. PP, no. 99, pp. 1–1, 2014.